RD_FA (R&D per Futuri Acceleratori)

M. Antonelli, G. Bencivenni, M. Bertani, O. Blanco (assegno di ricerca), M. Boscolo (Resp.), A. Ciarma (dottorando), E. De Lucia, D. Dominici, G. Felici, G. Morello, L. Pellegrino, M. Poli Lener, M. Rotondo, I. Sarra

RD_FA stands for R&D for Future Accelerators, it was initiated in 2017 by the CSN1. The activity is organized in Working Packages as follows:

- WP1: Fisica e simulazione
- WP2: Machine Detector Interface (M. Boscolo, convener)
- WP3: Pixel detectors
- WP4: RICH e TPC con MPGD
- WP5: Ultralight drift chamber
- WP6: Silicon microstrip tracking
- WP7: Micro-RWELL R&D
- WP8: Muon Collider R&D (M. Antonelli, convener)

For the year 2020 the LNF group was involved in WP2, WP7 and WP8. In the following we summarize the activity.

1 WP2: Machine Detector Interface for FCC-ee and FCC-hh

2 WP7:Micro-RWELL R&D

The µ-RWELL, fig.1, is a single-amplification stage resistive MPGD [1] that combines in a unique approach the solutions and improvements achieved in the last years in the MPGD field. The R&D on µ-RWELL aims to improve the stability under heavy irradiation while simplifying the construction procedures in view of an easy technology transfer to industry: a milestone for large scale applications in fundamental research at the future colliders and even beyond the HEP.
The detector is composed of two elements: the cathode, a simple FR4 PCB with a thin copper layer on one side and the µ-RWELL_PCB, the core of the detector. The µ-RWELL_PCB, a multi-layer circuit realized by means of standard photo-lithography technology, is composed of a well patterned single copper-clad polyimide (Apical®) foil acting as amplification element of the detector; a resistive layer, realized with a DLC film sputtered on the bottom side of the polyimide foil, as discharge limitation stage; a standard PCB for readout purposes, segmented as strip, pixel or pad electrodes.
Applying a suitable voltage between the copper layer and the DLC, the well acts as a multiplication channel for the ionization produced in the drift gas gap, fig.2. The charge induced on the resistive film is spread with a time constant [2, 3]

$$\tau = \rho c = \rho \frac{\epsilon_0 \epsilon_r}{t}$$

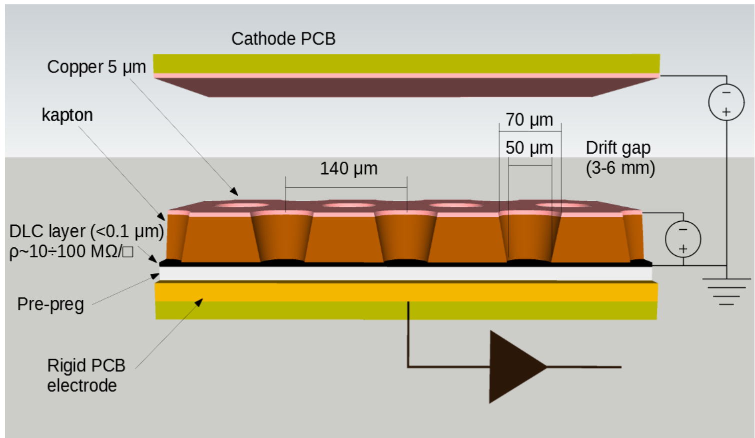

Figure 1: Layout of the µ-RWELL.

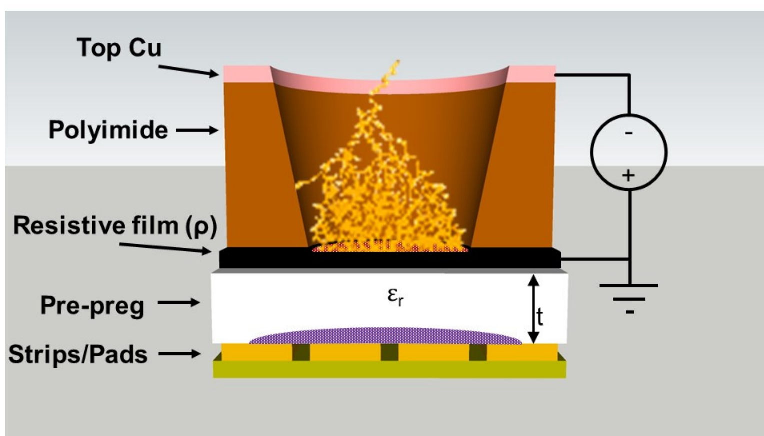

Figure 2: Principle of operation of the µ-RWELL.

being ρ the surface resistivity (in the following simply called resistivity), c the capacitance per unit area and t the distance between the resistive layer and the readout plane.
The spark suppression mechanism is similar to the one of the Resistive Plate Counters - RPCs, [4, 5, 6, 7]: the streamer created inside the amplification volume, inducing a large current flowing through the resistive layer, generates a localized drop of the amplifying voltage with an effective quenching of the multiplication process in the gas. This mechanism strongly suppressing the

discharge amplitude allows an operation of the detector at large gains ($\geq 10^4$) with a single amplification stage.

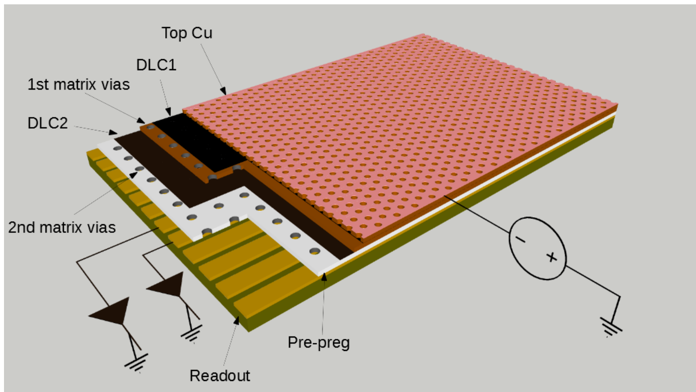

Figure 3: Sketch of the Double-Resistive layout.

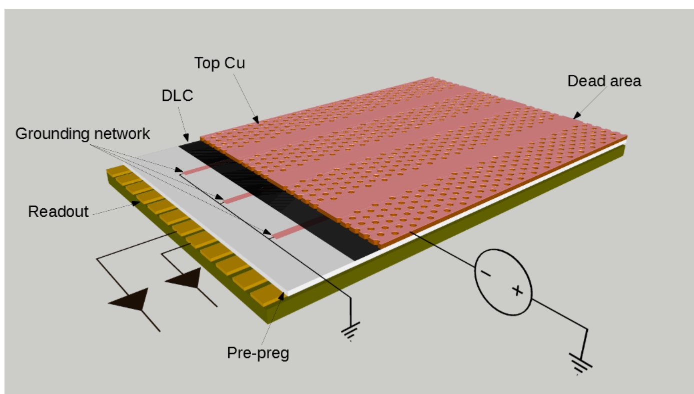

Figure 4: Sketch of the Silver-Grid layout.

A drawback, correlated with the Ohmic behaviour of the detector, is the reduced capability to stand high particle fluxes. Indeed a detector relying on a simple single-resistive layout suffers at high particle fluxes of a non-uniform response over its surface, more evident as the size of the detector increases. This effect depends on the distance between the particle incidence position and the detector grounding line. This limitation can be improved creating a high density ground network on the DLC.
Different high rate (HR) layouts have been implemented:

- the Double-Resistive Layer (DRL)
- the Silver-Grid (SG2++)

In the DRL layout (fig. 3) two vias matrices (density ¡1/cm2) in cascade connect the DLC films to ground. The DRL shows very good performance with no dead zone in the amplification stage, but

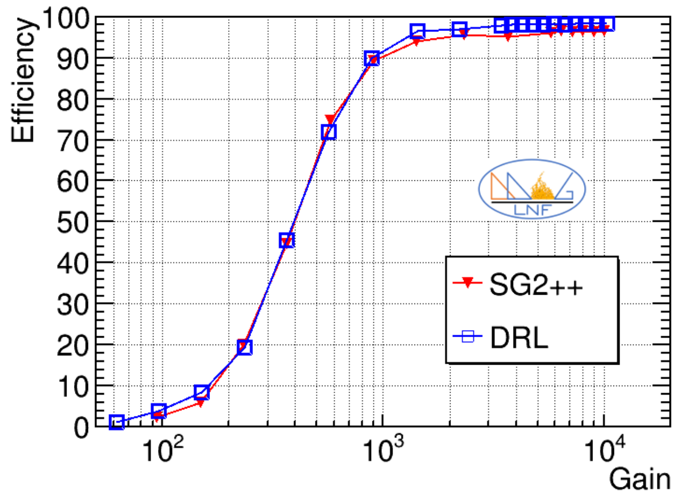

Figure 5: Efficiency as a function of the gas gain for the HR layouts.

has a complex manufacturing. In the SG layout, fig. 4, a copper grid (1 cm pitch) patterned on the DLC acts as the grounding system. The SG is simpler than the DRL because it uses a single DLC layer and does not require complex production steps (i.e. double matrix of vias), but it needs a tiny dead zone in the amplification stage above the grid.
The activity for the 2020 is focused on the HR performance in terms of efficiency and rate capability as measured at PSI beam lines.

2.1 Performance of the HR-layouts

The performance of the HR-layouts have been measured with pion at the πM1 of PSI. The experimental set-up used is composed of:

- two couple of plastic scintillators (up-stream/down-stream), providing the DAQ trigger;
- two external triple-GEM trackers equipped with 650 μm pitch X-Y strip read-out with analog APV25 front-end electronics [13], defining the particle beam with a spatial accuracy of the order of 100 μm;
- six μ-RWELL detectors based on different resistive layouts, equipped with 0.6×0.8 cm^2 pads and read-out with APV25 and current monitored.

The gaseous detectors have been operated with $Ar/CO_2/CF_4$ (45/15/40) gas mixture.
In fig. 5 the efficiency of the HR-layouts is reported as a function of the detectors gain. The measurement has been performed with a flux of $\sim$300 kHz/cm^2 π^- (350 MeV/c) and an average beam spot of 5×5 cm^2 (FWHM^2). The efficiency has been evaluated considering a fiducial area of 5×5 pads around the expected hit. At a gain of 5000 the DRL shows an efficiency of 98%, while SG2++ tends to an almost full efficiency of about 97%.

The rate capability of the HR-layouts has been measured at the PSI πM1 facility that provides a quasi-continuous high-intensity secondary beam with a fluence of $\sim10^7$ π^-/s and $\sim10^8$ π^+/s, for a momentum ranging between $270\div350$ MeV$/c$. This measurement can be considered

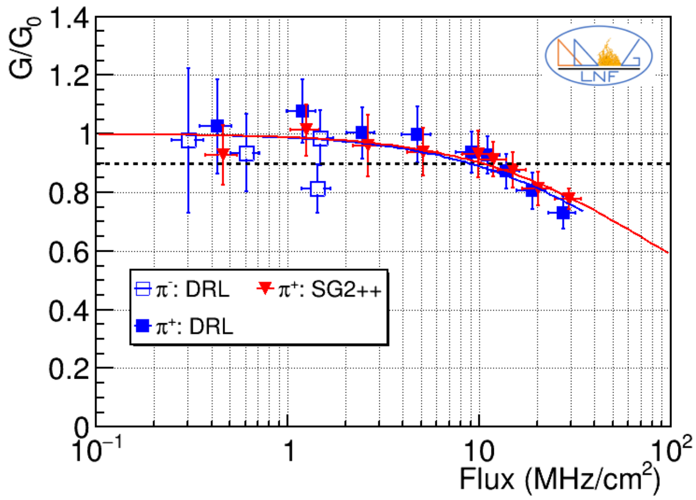

Figure 6: Normalized gas gain for the HR-layouts as a function of the pion flux. The function used to fit the points is the one derived in [1].

reliable because the dimension of the average beam spot is larger than the basic cells of all the HR prototypes. The result of this study is reported in fig. 6.
The low rate measurements ($\leq$1 MHz/cm^2) have been performed with the π^- beam, while the high intensity have been obtained with the π^+ beam. The detectors have been operated at a gain of about 5000. The particle rate has been estimated with the current drawn by the GEM, that owns a linear behaviour up to several tens of MHz/cm^2 [14]. The beam spot has been evaluated with a 2-D gaussian fit of the hits reconstructed on the X-Y plane for each detector.
The gain drop observed at high particle fluxes is correlated with the ohmic behaviour of the detectors due to the DLC film. The larger the radiation rate, the higher is the current drawn through the resistive layer and, as a consequence, the larger the drop of the amplifying voltage.
The proposed layouts show a rate capability up to 10 MHz/cm^2 with a detection efficiency of the order of 97÷98% that satisfy the stringent requirements for the detectors in the apparatus at the future accelerators FCC-ee/hh and CepC.

3 WP8: Muon Collider

4 List of Conference Talks in Year 2020

1. M. Giovannetti, The u-RWELL for high rate applications, INSTR20: Instrumentation for Colliding Beam Physics, Budker Institute of Nuclear Physics and Novosibirsk State University, Novosibirsk, Russia, 24-28 February, 2020.

5 Publications for the year 2020

1. G. Bencivenni *et al.*,“The u-RWELL for high rate applications,” JINST 15 (2020) C09034.

References

1. G. Bencivenni at al., *The micro-Resistive WELL detector: a compact spark-protected single amplification-stage MPGD*, JINST 10 (2015) P02008.

2. M.S. Dixit et al., *Simulating the charge dispersion phenomena in Micro Pattern Gas Detectors with a resistive anode*, Nucl. Instr. & Meth. **A 566** (2006) 281.

3. G. Bencivenni et al., *Performance of μ-RWELL detector vs resistivity of the resistive stage*, Nucl. Instr. & Meth. **A 886** (2018) 36-39.

4. Y. Pestov et al., *A spark counter with large area*, Nucl. Instr. & Meth. **93** (1971) 269.

5. R. Santonico, R. Cardarelli, *Development of Resistive Plate Counters*, Nucl. Instr. & Meth. **A 377** (1981) 187.

6. M. Anelli et al., *Glass electrode spark counters*, Nucl. Instr. & Meth. **A 300** (1991) 572.

7. P. Fonte et al., *Advances in the Development of Micropattern Gaseous Detectors with Resisitve Electrodes*, Nucl. Instr. & Meth. **A 661** (2012) 153.

8. A. Ochi et al., *Carbon sputtering Technology for MPDG detectors*, Proceeding of Science (TIPP2014) 351.

9. G. Morello et al., *Advances on micro-RWELL gaseous detector*, Proceeding of Science (BORMIO2017) 002.

10. Y. Zhou et, al, *News on DLC Coatings, contribution to the RD51 Collaboration Meeting and the topical workshop on MPGD Stability, 18-22 June 2018, Technical University of Munich - Munich, Germany. https://indico.cern.ch/event/709670/timetable/#20180622.detailed.*

11. G. Bencivenni et al., *A triple GEM detector with pad readout for high rate charged particle triggering*, Nucl. Instr. & Meth. **A 488** (2002) 493.

12. C. Richter et al, *Absolute electron transfer efficiency of GEM*, Nucl. Instr. & Meth. **A 461** (2001) 38.

13. M. Raymond et al., *The APV25 0.25 m CMOS readout chip for the CMS tracker*, IEEE Nucl. Sci. Symp. Conf. Rec. **2** (2000) 9/113.

14. M. Alfonsi et al., *High rate particle triggering with triple-GEM detector*, Nucl. Instr. & Meth. **A 518** (2004) 116.